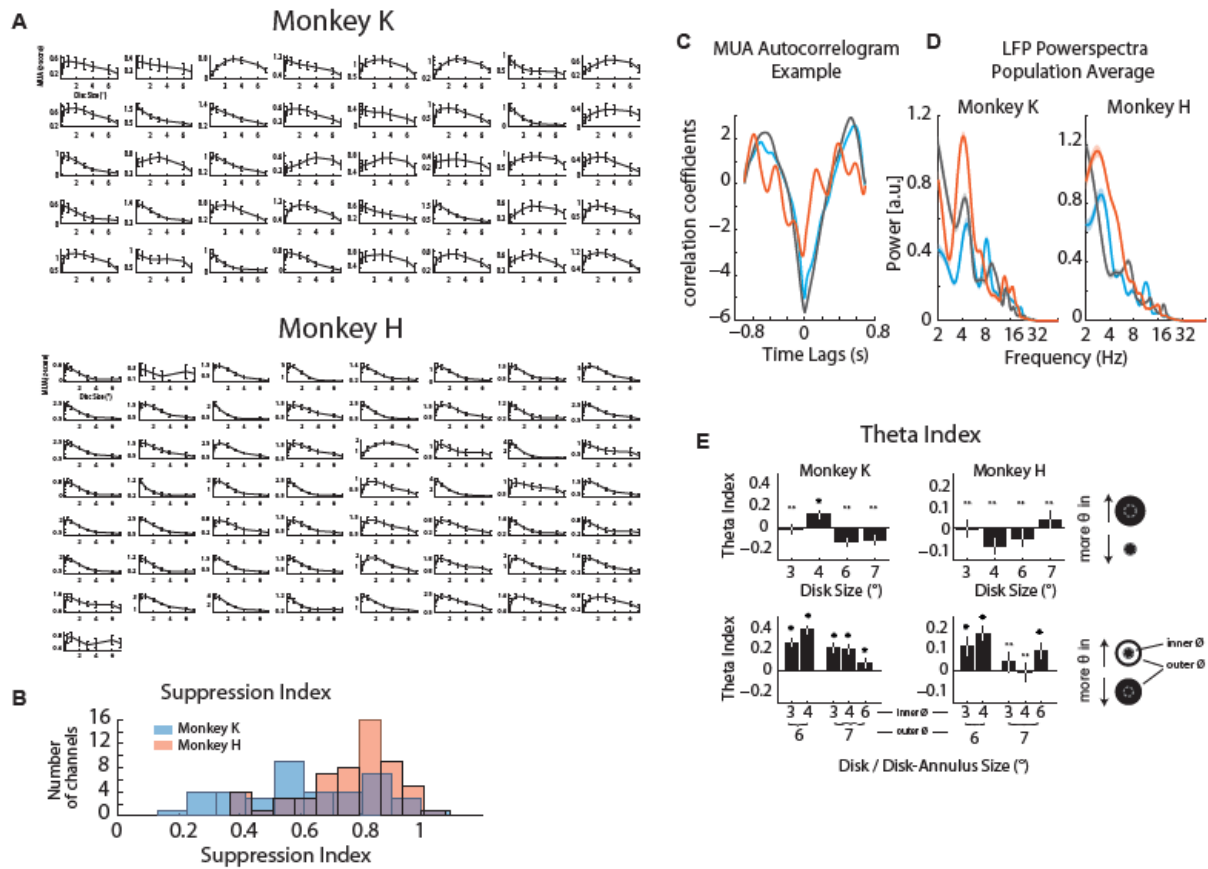


## Supplemental Information

### Supplemental Figure Legends

Fig. S1



**Figure S1. Related to Figure 1. Surround suppression and theta oscillations.**

- (A) Size tuning curves of all included channels (average across trials) from monkey K (top panel) and monkey H (lower panel).
- (B) Distribution of SI values from monkey K (blue, mean =  $0.62 \pm 0.03$ ,  $n = 40$ ) and monkey H (red, mean =  $0.77 \pm 0.02$ ,  $n = 57$ ).
- (C) Example MUA autocorrelogram from the same channel as in Figure 1B-C with the same color conventions (small  $2^\circ$  disk (blue); large  $6^\circ$  disk (gray);  $2^\circ$  disk with 4- $6^\circ$  annulus (orange)). Note the oscillation in the disk-annulus condition only (orange) that resembles the findings of the spectral analysis in Figure 1B.
- (D) Population average of LFP powerspectra across channels for monkey K (left panel) and H (right panel), same color convention as in (C) and in Figure 1B-C. Note the presence of a peak in the theta range and that strongest theta power is found in the disk-annulus condition (orange).
- (E) Upper Row: Distributions of theta indices comparing the theta power of a  $2^\circ$  disk (diameter), roughly corresponding to the RF center, vs. larger disks also stimulating the RF surround ( $3^\circ$ ,  $4^\circ$ ,  $6^\circ$ ,  $7^\circ$  in diameter). Positive values indicate higher theta power for the larger disk (presence of inhibition). Note that no theta peak was visible in the powerspectra for both small and large disks (Figure 1) indicating that higher power values represent unspecific over-all power shifts.

Lower Row: Distributions of theta indices comparing the theta power of large disks and disk-annulus stimuli with the same outer diameter, i.e. same spatial extent into suppressive surround. Positive values indicate higher theta power for the disk-annulus stimuli.

Fig.S2

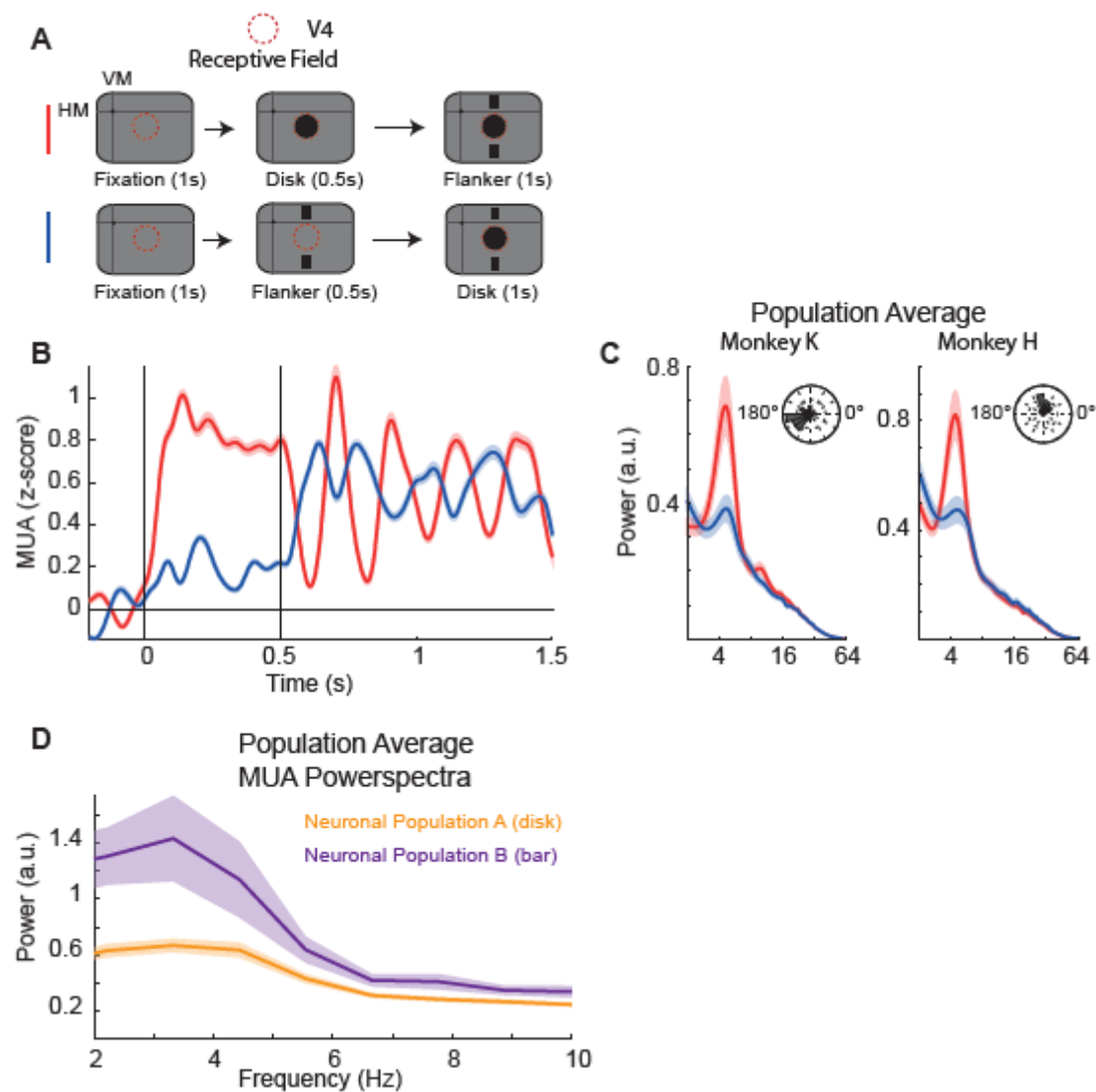


**Figure S2. Related to Figure 2. Stimulus timing and location controls phase.**

- (A) Experimental design involving passive viewing disk-flanker stimulation providing the data shown in B-C. After 1s of fixation either the disk (in RF center, red) or the flanker (in RF suppressive surround, blue) appeared first, followed by the respective other stimulus.
- (B) MUA responses from one example channel of monkey K to the two different stimulation conditions (averaged across trials), same color conventions as in (A).
- (C) Population powerspectra of monkey K (left panel) and monkey H (right panel) with phase plots showing the channel-wise theta phase-differences between the two conditions of monkey K (left panel) and monkey H (right panel) across channels (mean:  $-168.6 \pm 6.7^\circ$ ,  $n = 41$  for monkey K; mean:  $93.8 \pm 7.3^\circ$ ,  $n = 57$ ), same color conventions as in (A).
- (D) Population average powerspectra across MUA channels of the task involving the sequential presentation of disk and bar as displayed in **Figure 2**.

Figure S3

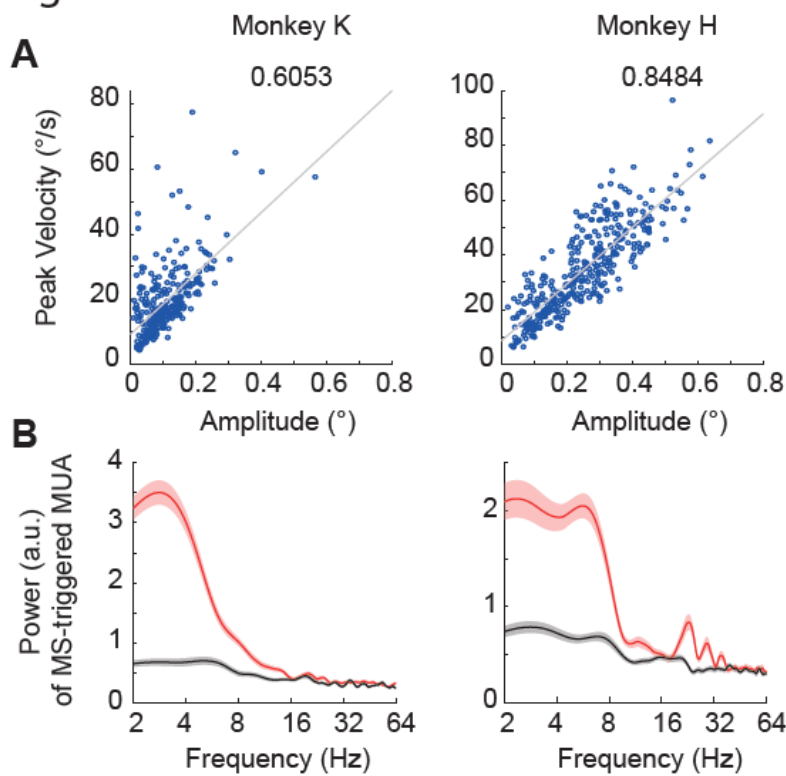


**Figure S3. Related to Figure 3. Microsaccade main sequence and MS-triggered MUA powerspectra**

- (A) Main sequence of microsaccades (MS) for monkey K (left) and H (right) showing the relation of amplitude and peak velocity of each MS and the respective correlation values across MS.
- (B) Powerspectra of MS-triggered MUA computed after MS onset for monkey K (left) and H (right) showing the actual data (red) and trial-shuffled control data (gray).

Fig. S4

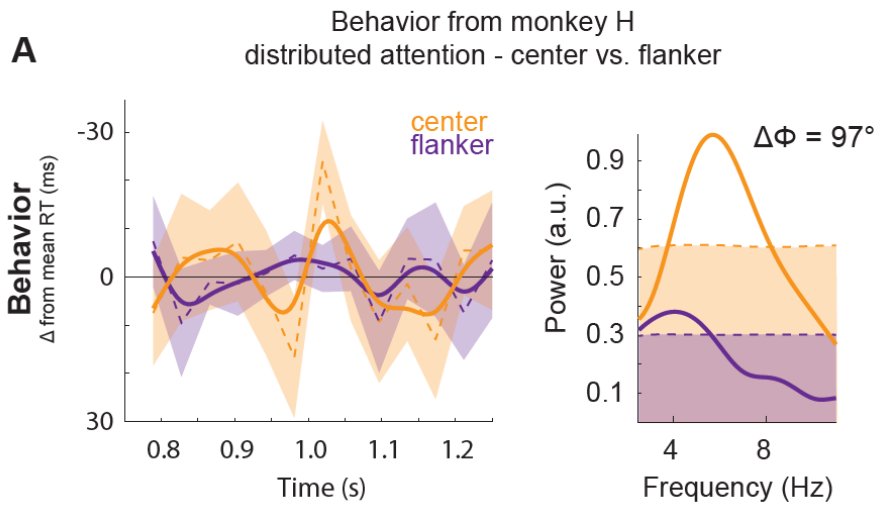


**Figure S4: Reaction time data of Monkey H.**

(A) Left panel showing the reaction time (as deviation from mean) as a function of target delay for the distributed attention condition in response to the center (solid line) and flanker target position (dashed line). Non-smoothed RT data shown as thin dashed lines, shadings around lines depict SEM. Right panel depicts powerspectra of the respective RT data and their phase difference ( $97^\circ$ ), shadings represent 95% confidence intervals based on shuffled surrogate data.

Fig. S5

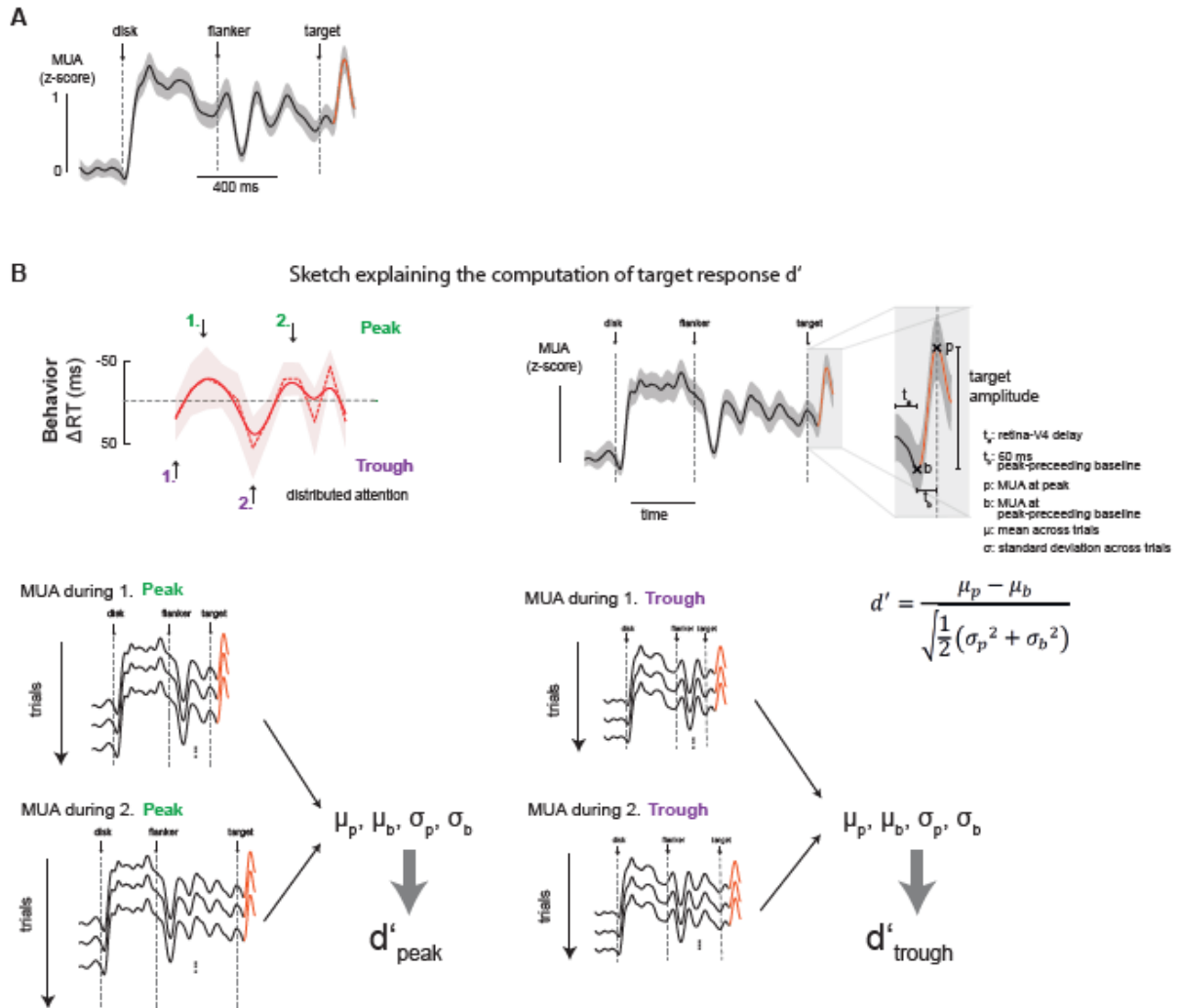


**Figure S5. Related to Figure 6. MUA target response and the computation of  $d'$ .**

(A) Example MUA channel, averaged across trials, recorded during the distributed attention task where the target presentation falls onto a trough / rising part of the ongoing oscillation. Compare to Figure 6A.

(B) Sketch illustrating the computation of the  $d'$  quantifying the target response. Upper left panel shows the RT trace of monkey K highlighting the peaks and troughs and the corresponding SOA conditions that were used to analyze MUA and its target responses during the distributed attention task. Upper right panel explains how the quantification of target responses and  $d'$  was calculated. The peak amplitude was defined as the amplitude difference between the peak and the baseline that preceded the peak by 60 ms. It was then related to its variation across trials as shown in the  $d'$  equation. The lower panels illustrate that the target responses were quantified across trials for the selected RT peak and trough SOAs.